Cell Host & Microbe
Article

Microbiota-Derived Hydrogen Fuels *Salmonella* Typhimurium Invasion of the Gut Ecosystem

Lisa Maier,[1] Rounak Vyas,[3] Carmen Dolores Cordova,[1] Helen Lindsay,[3] Thomas Sebastian Benedikt Schmidt,[3] Sandrine Brugiroux,[2] Balamurugan Periaswamy,[1] Rebekka Bauer,[1] Alexander Sturm,[1] Frank Schreiber,[4] Christian von Mering,[3] Mark D. Robinson,[3] Bärbel Stecher,[2] and Wolf-Dietrich Hardt[1,*]
[1]Institute of Microbiology, ETH Zürich, CH-8093 Zurich, Switzerland
[2]Max-von-Pettenkofer Institute, Ludwig-Maximilians-Universität Munich, 80336 Munich, Germany
[3]SIB Swiss Institute of Bioinformatics, University of Zurich, CH-8057 Zurich, Switzerland
[4]Department of Environmental Microbiology, Eawag and Department of Environmental Systems Sciences, ETH Zurich, CH-8600 Dübendorf, Switzerland
*Correspondence: wolf-dietrich.hardt@micro.biol.ethz.ch
http://dx.doi.org/10.1016/j.chom.2013.11.002

SUMMARY

The intestinal microbiota features intricate metabolic interactions involving the breakdown and reuse of host- and diet-derived nutrients. The competition for these resources can limit pathogen growth. Nevertheless, some enteropathogenic bacteria can invade this niche through mechanisms that remain largely unclear. Using a mouse model for *Salmonella* diarrhea and a transposon mutant screen, we discovered that initial growth of *Salmonella* Typhimurium (*S*. Tm) in the unperturbed gut is powered by *S*. Tm *hyb* hydrogenase, which facilitates consumption of hydrogen (H_2), a central intermediate of microbiota metabolism. In competitive infection experiments, a *hyb* mutant exhibited reduced growth early in infection compared to wild-type *S*. Tm, but these differences were lost upon antibiotic-mediated disruption of the host microbiota. Additionally, introducing H_2-consuming bacteria into the microbiota interfered with *hyb*-dependent *S*. Tm growth. Thus, H_2 is an Achilles' heel of microbiota metabolism that can be subverted by pathogens and might offer opportunities to prevent infection.

INTRODUCTION

The mammalian intestine is densely colonized by microorganisms, collectively referred to as microbiota (Ley et al., 2008). The microbiota feature a network of metabolic activities facilitating efficient breakdown of complex diet- and host-derived carbohydrates to short-chain fatty acids (SCFAs), hydrogen (H_2), and carbon dioxide (Fischbach and Sonnenburg, 2011; Flint et al., 2008). Microbial fermentation products are subsequently consumed by crossfeeding secondary fermenters, absorbed by the host, or released into the environment. Gut ecosystem invasion is defined herein as the initial growth phase of a pathogen (or any other newcomer) in the host's intestine. At this stage, the intestinal mucosa appears healthy, and the microbiota is (still) intact and limits nutrient availability. This prohibits growth of most newly arriving bacteria. Despite the scarce nutrient availability, enteropathogens can invade the gut ecosystem. Yet, the factors enabling "gut ecosystem invasion" by enteropathogens remain unclear.

The human food-borne pathogen *Salmonella* Typhimurium (*S*. Tm), a causative agent of diarrhea, can grow up in this nutrient-depleted environment to high numbers and cause disease. Animal experiments established that gut luminal pathogen densities must rise to 10^7–10^8 cfu per gram of stool before enteropathy is elicited (Ackermann et al., 2008; Barthel et al., 2003). As inoculum sizes as low as 10^3–10^5 bacteria suffice for causing diarrheal disease in humans (Food and Agriculture Organization of the United Nations, 2002), we speculated that *S*. Tm can grow initially in the face of an intact microbiota and a healthy gut. The mechanisms fostering *S*. Tm growth in this densely colonized niche are still enigmatic. Such mechanisms can be studied using "low complex microbiota" (LCM) mice, which are permissive for gut luminal *S*. Tm growth (Figure S1A available online; Stecher et al., 2010). LCM mice are ex-germ-free mice which had originally been colonized with strains of the "Altered Schaedler Flora" (Experimental Procedures, Figures S1A and S1E) and permit gut luminal colonization by inocclum sizes as small as 200 colony-forming units (Endt et al., 2010; Stecher et al., 2010). During the first 2 days, there are no signs of enteropathy, and the pathogen grows up to 10^6–10^8 cfu/g stool (gut ecosystem invasion). Mucosal inflammation is elicited at days 3–4 postinfection when the pathogen reaches a final density of 10^8–10^{10} cfu/g stool (Stecher and Hardt, 2011; Figure S1A). Thus, LCM mice should provide a unique model for analyzing all phases of host gut colonization, including gut ecosystem invasion.

RESULTS

Screening for *S*. Tm Mutants Impaired in Early Gut Ecosystem Invasion

To identify *S*. Tm genes required for any stage of gut luminal colonization, we performed an unbiased competitive infection experiment. Specifically, we constructed a set of 500 *S*. Tm transposon mutants (Badarinarayana et al., 2001) and infected LCM mice via the orogastric route. The input pools were

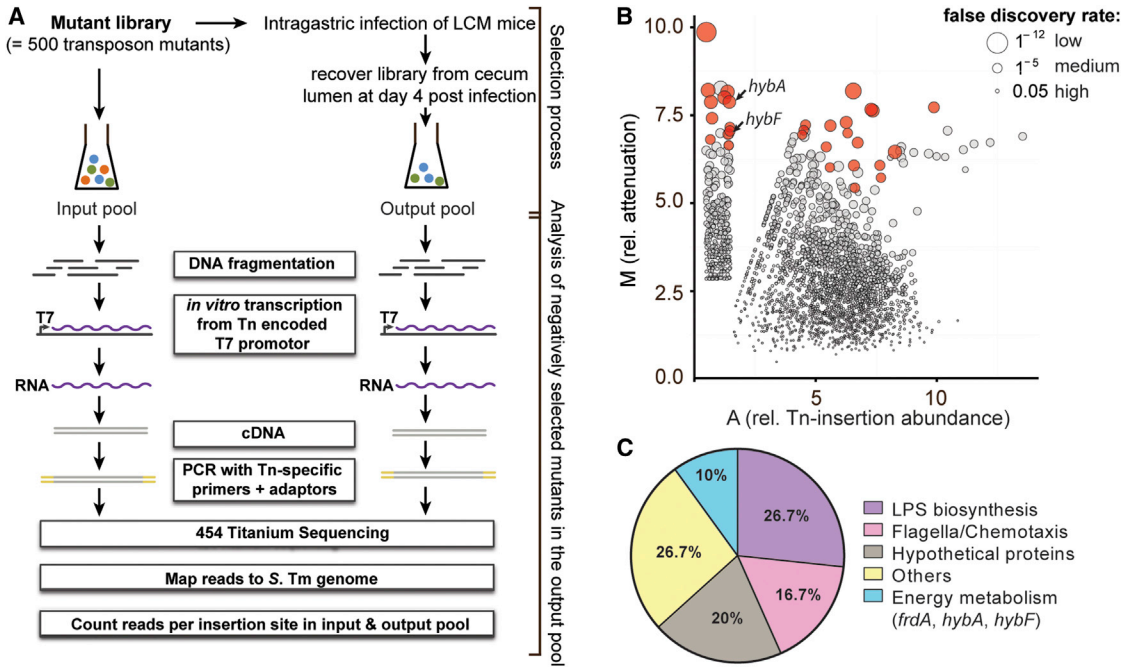

Figure 1. Signature-Tagged Mutagenesis-like Screen for *S.* Tm Genes Required for Gut Lumen Colonization In Vivo

(A) Experimental strategy: 500 randomly generated transposon (Tn) mutants were pooled, and six LCM mice were infected by gavage (Experimental Procedures; Figures S1B–S1E). At day 4 p.i. mutant pools were isolated from the cecum lumen. Next-generation sequencing of transposon-flanking regions using the Tn-encoded T7 promoter permitted identification of Tn insertion sites and of Tn insertions affecting pathogen fitness in the gut lumen.

(B) Statistical analysis of the mutant phenotypes. M/A plot showing the relative attenuation (log_2 fold change in read counts between input and output pools) for each Tn mutant plotted against the relative Tn insertion abundance (= average log_2 counts per million reads, multiplied by the normalized library size to account for differences in the total number of reads sequenced in each sample). A large dot size represents a low false discovery rate (FDR). The 30 most attenuated mutants containing the Tn insertion within a gene are highlighted in red (Table S1). This cutoff was reasonable, as several genes tested in earlier experiments with a C.I. of $0.8 < x < 1.2$ displayed FDR values of $0.005–1^{-5}$.

(C) Functional classification of the 30 most-attenuated Tn insertion mutants.

See also Figure S1 and Table S1.

compared to mutant pools in the cecum lumen at day 4 after infection using transposon-directed insertion-site sequencing (TraDIS; Chaudhuri et al., 2013; van Opijnen and Camilli, 2013), and mutations compromising gut-luminal colonization were identified (six independent animals, two experiments; Figures 1A and S1B–S1E). Transposon insertions in 30 genes reduced gut-luminal abundance of the mutant in all six mice and scored with high confidence ($p \leq 1.3 \times 10^{-5}$; highlighted in red in Figure 1B; Table S1). Almost half of these identified genes were involved in chemotaxis or in flagellar or LPS biosynthesis (Figure 1C). These are well-established *S.* Tm virulence factors required for growth and survival in the inflamed gut (Allen-Vercoe and Woodward, 1999; Chaudhuri et al., 2013; Craven, 1994; Ilg et al., 2009; Stecher et al., 2008; Stecher et al., 2004). These genes likely contribute to expansion/maintenance of the pathogen population at days 3 and 4 of the experiment and confirmed the robustness of our experimental approach. We also identified three genes involved in anaerobic energy metabolism (Figure 1C), *frdA*, the first gene of the operon encoding the fumarate reductase complex, *hybA* and *hybF*. The latter two genes encode subunits of a NiFe-hydrogenase known to consume molecular hydrogen as an electron source in anaerobic environments, thus powering microbial growth ("energy conservation"; Figure S2A) (Lamichhane-Khadka et al., 2010; Maier et al., 2004; Zbell et al., 2008). As H_2 is produced by primary fermenters of the microbiota (*not* the host; Fischbach and Sonnenburg, 2011; Flint et al., 2008), this provided hints that *S.* Tm may capitalize on this microbiota-derived metabolite during some stage of intestinal colonization.

Hydrogen Consumption by *S.* Tm Is Only Required during the Initial Phase of Gut Ecosystem Invasion

In order to verify the role of hydrogenases during gut infection, we constructed site-directed mutants (Figure S2B; Supplemental Experimental Procedures). In competitive infections, the *hyb* mutant (*S.* Tm^{hyb}; *hybBCAhypO*, which lacks all structural genes of the *hyb* hydrogenase) displayed a pronounced growth defect compared to the isogenic wild-type strain (≈100-fold; $p < 0.05$; Figure 2). This was corrobated by *hyb* expression in the gut lumen (Figure S2D). Interestingly, the growth defect of *S.* Tm^{hyb} was restricted to the first day of the experiment when pathogen loads were still low ($\leq 10^8$ cfu/g stool) and no signs of mucosal inflammation were observed (Figures 2B–2D). Thereafter, the competitive index did not drop any further (Figure 2A). These data indicate that *S.* Tm requires *hyb* only in the initial phase of gut ecosystem invasion, but not at later stages of the infection, and that this initial stage (days 0–1) is mechanistically distinct.

Further experiments excluded major contributions of two alternative H_2-consuming hydrogenases encoded in the *S*. Tm genome (Figure S2B; Supplemental Experimental Procedures). Disrupting the two alternative hydrogenases yielded no defects in gut ecosystem invasion, and the hydrogenase triple mutant (*S*. Tm^{hyd3}) displayed the same in vivo growth defect as did *S*. Tm^{hyb} (Figures S3A and S3B). Thus, while *hyb* is necessary for robust pathogen growth in the host's intestine, the other two hydrogenases contribute little. This was further supported by complementation (Figure S3B). Furthermore, the gut ecosystem invasion defect of the hydrogenase mutant was independent of the inoculum size and also observed upon gavage of 5×10^3 cfu (data not shown; standard inoculum size = 5×10^7 cfu; Experimental Procedures). Finally, in vitro experiments in anaerobic broth culture verified that the growth defect of *S*. Tm^{hyd3} was only observed in the presence of H_2, but not in its absence (Figures S4A and S4B). In conclusion, these data confirmed the pivotal importance of *hyb* for H_2-dependent *S*. Tm growth.

Our initial data suggested that the *hyb* hydrogenase may fuel pathogen growth during gut ecosystem invasion, i.e., the first 24 hr p.i. (Figure 2A). At this stage the pathogen grows in the face of the resident microbiota (which presumably still produces H_2) and overt inflammation is not yet triggered (Figures S1A and 2B–2D). To further substantiate the need for hydrogenases in the noninflamed gut, we performed competition experiments in the avirulent strain background. The isogenic *S*. Tm mutant (*S*. Tm^{avir}; Δ*invG*Δ*sseD*; Supplemental Experimental Procedures) colonizes the gut but remains "locked" in gut ecosystem invasion phase of the infection, as it lacks two key virulence factors and therefore cannot elicit overt mucosal inflammation (Hapfelmeier et al., 2005; Stecher et al., 2007). To this end, we constructed a hydrogenase-deficient mutant in the *S*. Tm^{avir} background (*S*. $Tm^{avir\ hyd3}$). First, we tested this strain's capacity to grow up in the gut of LCM mice. In competitive infections, *S*. $Tm^{avir\ hyd3}$ displayed a pronounced colonization defect on day 1 p.i. but no further decrease from day 1 to day 4 p.i. (Figure 3). These results were strikingly similar to those obtained in the wild-type *S*. Tm strain background (compare Figure 2A and Figure 3A) and verified that hydrogenases are indeed only required during gut ecosystem invasion, whether inflammation is triggered or not. Accordingly, intravenous infection experiments confirmed that hydrogenases are not needed for growth at systemic sites (Figure S3C). This further supported the notion that gut ecosystem invasion is a distinct step in host intestinal colonization, which prepares the ground for subsequent stages of the infection.

Microbiota-Derived H_2 Is Responsible for the Competitive Defect of *S*. Tm Hydrogenase Mutants during Early Gut Invasion

Next, we addressed the role of the resident microbiota in *hyb*-dependent gut ecosystem invasion. As the microbiota is considered to be the source of all available H_2, presence of a H_2 producing microbial community should be required for hydrogen-dependent pathogen growth. To this end, we measured H_2 concentrations in freshly dissected ceca ex vivo using a hydrogen microsensor (Experimental Procedures). In germ-free mice lacking all associated microbiota, no H_2 was measurable in the cecum lumen (<2 μM, Figure 4A), and *S*. $Tm^{avir\ hyd3}$ did not display any competitive growth defect (Figures 4B, 4E, and 4F). In contrast, the cecum of LCM mice harbored high levels of H_2 (Figure 4A). This was strikingly similar to the levels of H_2 in the cecum of CON mice, which harbor a "normal," complex microbiota (Figure 4A), as well as the large intestine of humans and diverse animal species (Table S3). With a K_M value of the *S*. Tm hydrogenase activity of 2.1 μM (Maier et al., 2004), these data verified microbiota-derived H_2 as a possible energy source during gut ecosystem invasion in vivo. Indeed, the competitive growth defect of *S*. Tm^{hyd3} in CON mice was comparable to that of LCM mice (Figure 4C and Figure 4D, left side; Figures 4E and 4F). As a complementary approach, we tested the effect of antibiotic pretreatment, a procedure known to reduce microbiota abundance by >10-fold, shift the microbiota composition, and increase metabolite availability in the large intestinal lumen (e.g., carbohydrates like fucose and sialic acids, both accessed by *S*. Tm for intestinal expansion) (Ng et al., 2013; Willing et al., 2011). This should alleviate the need for *hyb*-dependent growth. Indeed, microbiota disruption by streptomycin pretreatment abrogated the competitive growth defect of *S*. Tm^{hyd3} in both LCM and CON mice (Figure 4C and Figure 4D, right side; Figures 4E and 4F). Conversely, microbiota transplantation from LCM mice to another gnotobiotic mouse model (VLCM mice; yield just a small C.I. for *S*. $Tm^{avir\ hyd3}$) reduced the colonization efficiency of *S*. $Tm^{avir\ hyd3}$ in competitive infections (Figures S4C and S4D). Finally, we quantified the total gut luminal population sizes achieved by a hydrogenase-deficient *S*. Tm strain. In both LCM and CON mice, *S*. $Tm^{avir\ hyd3}$ yielded significantly lower total intestinal *Salmonella* loads than the parental strain (*S*. Tm^{avir}; Figure 5). Collectively, these findings support the pivotal role of microbiota-derived H_2 during gut ecosystem invasion by *S*. Tm.

Genes Encoding for H_2-Producing Enzymes Are Abundant in Microbial Gut Metagenomes

Metagenome analyses were performed to assess the potential availability of H_2 in different hosts. Microbial H_2-metabolizing pathways, which are essential for efficient fermentation, are thought to rely on three classes of enzymes: NiFe-hydrogenases, FeFe-hydrogenases, and HmD-like enzymes (Schwartz and Friedrich, 2006). Based on the presence of sequences for one or more of these enzymes, all publically available gut metagenomes showed evidence for H_2-generating pathways (Tables 1 and S4; Experimental Procedures). The same was true for the cecal microbiota of the LCM mice studied here (MG-Rast accession numbers 4535626.3 and 4535627.3). This was well in line with published work on H_2 levels measured in the intestinal tract of animals and man (Table S3) and verified that H_2 production indeed represents a universal metabolic feature of the complex microbiota (and our simplified LCM model). However, the absolute H_2 levels may vary depending on host species or diet. Thus, the balance between H_2 production (i.e., by primary fermenters; Carbonero et al., 2012) and "H_2-loss" by H_2-consuming species of the microbiota (e.g., the methanogens like *Methanobrevibacter smithii*, the reductive acetogens like *Blautia hydrogenotrophica*, and sulfate-reducing bacteria like *Desulfobacter* spp. or *Desulfovibrio* spp.; Carbonero et al., 2012), as well as by diffusion, blood-mediated transport, and

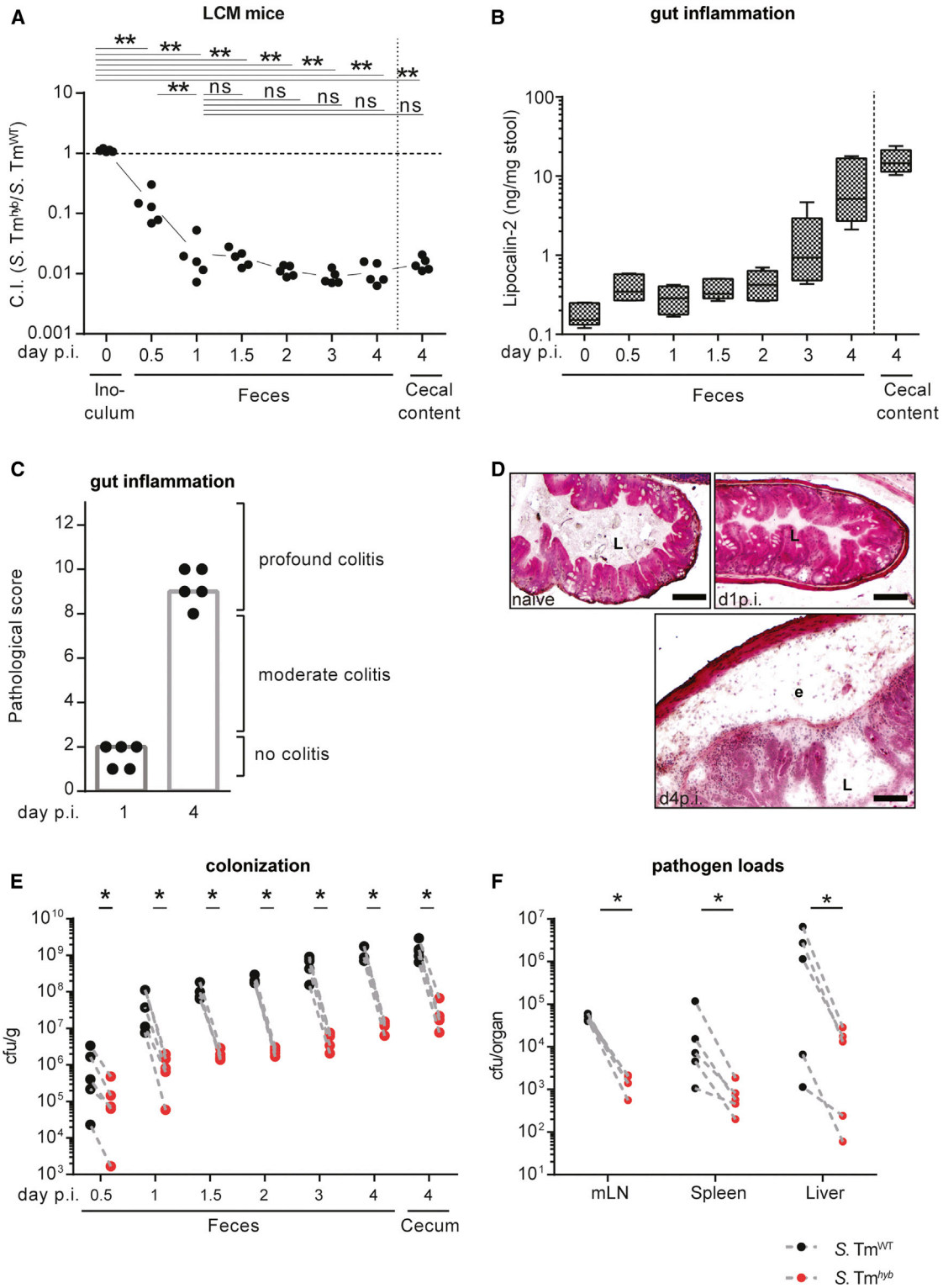

Figure 2. *S.* Tm *hyb*-Hydrogenase Mutant Shows Defective Gut Ecosystem Invasion

(A) Mice were infected with 1:1 mixtures (5×10^7 cfu by gavage) of the *hyb*-hydrogenase mutant and the isogenic hydrogenase-proficient background strain *S.* Tm^{WT}. Fecal loads of both strains were determined by plating and served to calculate of the competitive indices (C.I.s; Experimental Procedures). C.I. experiments were performed in five naive LCM mice. ns, not significant ($p \geq 0.05$), **$p < 0.01$; Mann-Whitney U test.

(B) Lipocalin-2 ELISA monitoring the onset of inflammation during the course of the experiment. Box and whiskers plot: the box indicates first and third quartiles, and whiskers denote minimal and maximal measurement readings.

(legend continued on next page)

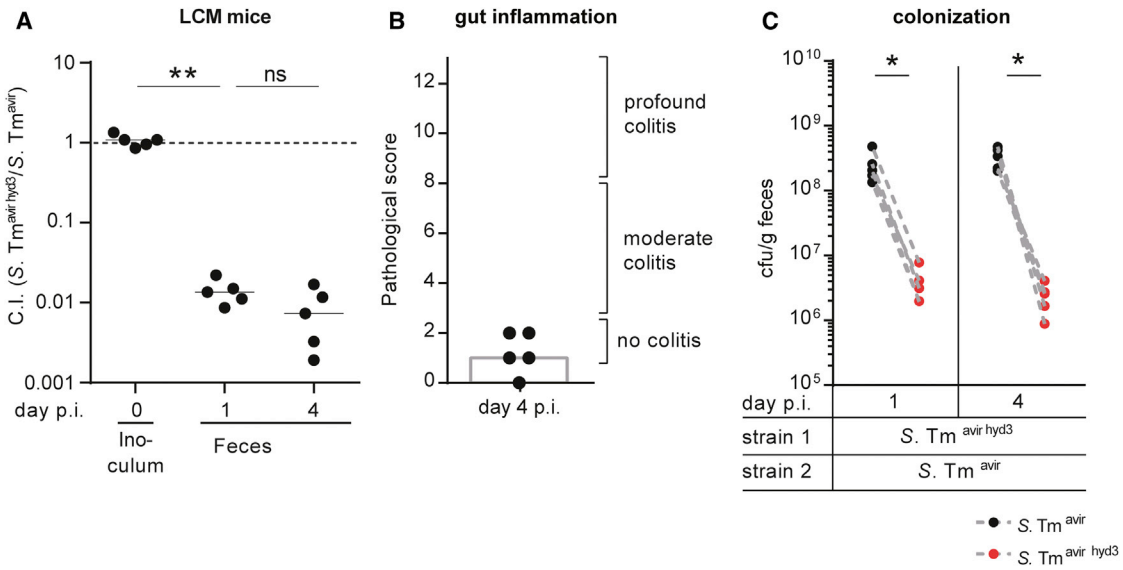

Figure 3. *S.* Tm Only Profits from H_2 during the Initial, Noninflammatory Phase of Gut Ecosystem Invasion

(A) C. I. experiments were performed in five naive LCM mice to test in vivo fitness of *S.* $Tm^{avir\ hyd3}$. ns, not significant ($p \geq 0.05$), **$p < 0.01$; Mann-Whitney U test.

(B) Pathological scores of the cecal mucosa at day 4 p.i. Cecal tissue sections from the competitive infection experiment shown in (A) were stained with HE and scored for inflammation.

(C) Fecal loads of *S.* $Tm^{avir\ hyd3}$ and *S.* Tm^{avir} at day 1 and day 4 p.i. were determined by differential plating. *$p < 0.05$, one-tailed Wilcoxon matched pairs signed rank test on paired data (dashed lines).

See also Figure S3.

exhalation, may dictate the efficiency of gut ecosystem invasion by incoming enteropathogens. As nutrition can affect gut microbiome richness and hydrogen availability (Cotillard et al., 2013; Le Chatelier et al., 2013), infection risks may depend in part on dietary habits.

Addition of an H_2 Consumer Can Interfere with *hyb*-Dependent *S.* Tm Growth

Due to their simplified species composition, the LCM mice offer a unique opportunity to manipulate functional features of the microbiota, e.g., by adding species or shifting the intestinal H_2 balance. To this end, we precolonized LCM mice with an additional "H_2 consumer," *S.* Tm^{avir} (Figure 6A). Control mice were precolonized with *S.* $Tm^{avir\ hyd3}$, a *S.* Tm strain which cannot consume hydrogen. In subsequent competive infection experiments, hydrogenases proved to be of greater importance for gut ecosystem invasion in the control mice than in the mice precolonized with *S.* Tm^{avir} ($p < 0.05$; *S.* $Tm^{avir\ hyd3}$ versus *S.* Tm^{avir}; Figures 6B and S5). Thus, pathogen colonization could be thwarted by introducing a H_2 consumer. This further supported the key role of H_2 for the initiation of *S.* Tm infection.

DISCUSSION

Our findings establish gut ecosystem invasion as a critical step of the orogastric *S.* Tm infection. During this initial phase of the infection, pathogen growth in the gut relies at least in part on metabolites provided by the microbiota. This differs markedly from the interactions observed later (i.e., during expansion/maintenance), when the host's mucosal immune response fuels pathogen growth and suppresses the microbiota (Kaiser et al., 2012; Winter et al., 2013). Thus, colonization of the host's gut comprises different phases featuring distinct sets of positive and negative interactions. The interactions between the pathogen, the microbiota, and the host are clearly more complex than previously anticipated.

Gut ecosystem invasion by *S.* Tm relies on H_2. This is true for mice harboring two different microbiotas of reduced complexity (LCM mice used thoughout most of this study; VLCM mice used in Figures S4C and S4D) or animals with a normal SPF microbiota, alike (Figures 4D–4F and 5B). In contrast, intravenous infections did not yield any evidence for H_2-dependent pathogen growth at systemic sites (Figure S3C). At first sight, this seems

(C and D) Histopathological evaluation of HE-stained cecal sections (L, intestinal lumen; e, edema in submucosa) of these mice. The HE-stained cecal tissue for day 1 p.i. was taken from the experiment shown in Figure S3A (1:1 infection with *S.* Tm^{WT} and *S.* Tm^{hyb}). Scale bar, 100 μm. This demonstrated that mucosal inflammation was elicited at days 3–4 postinfection, as confirmed by pathological scoring.

(E) The bacterial loads of *S.* Tm^{WT} (black symbols) and *S.* Tm^{hyb} (red symbols) populations were monitored in the feces during the course of the infection and in the cecal content at the end of the experiment. These data verify the distinct colonization defect of *S.* Tm^{hyb} during the first day of infection.

(F) Pathogen loads of *S.* Tm^{WT} (black symbols) and *S.* Tm^{hyb} (red symbols) in systemic organs at day 4 p.i. *$p < 0.05$, one-tailed Wilcoxon matched pairs signed rank test on paired data (dashed lines). Please note that the reduced loads of *S.* Tm^{hyb} in lymph nodes, spleens, and livers were most likely attributable to the reduced seeding from the intestinal lumen (which must have occurred after the initial *hyb*-dependent growth in the gut; see Figure S3C, below).

See also Figure S2 and Table S2.

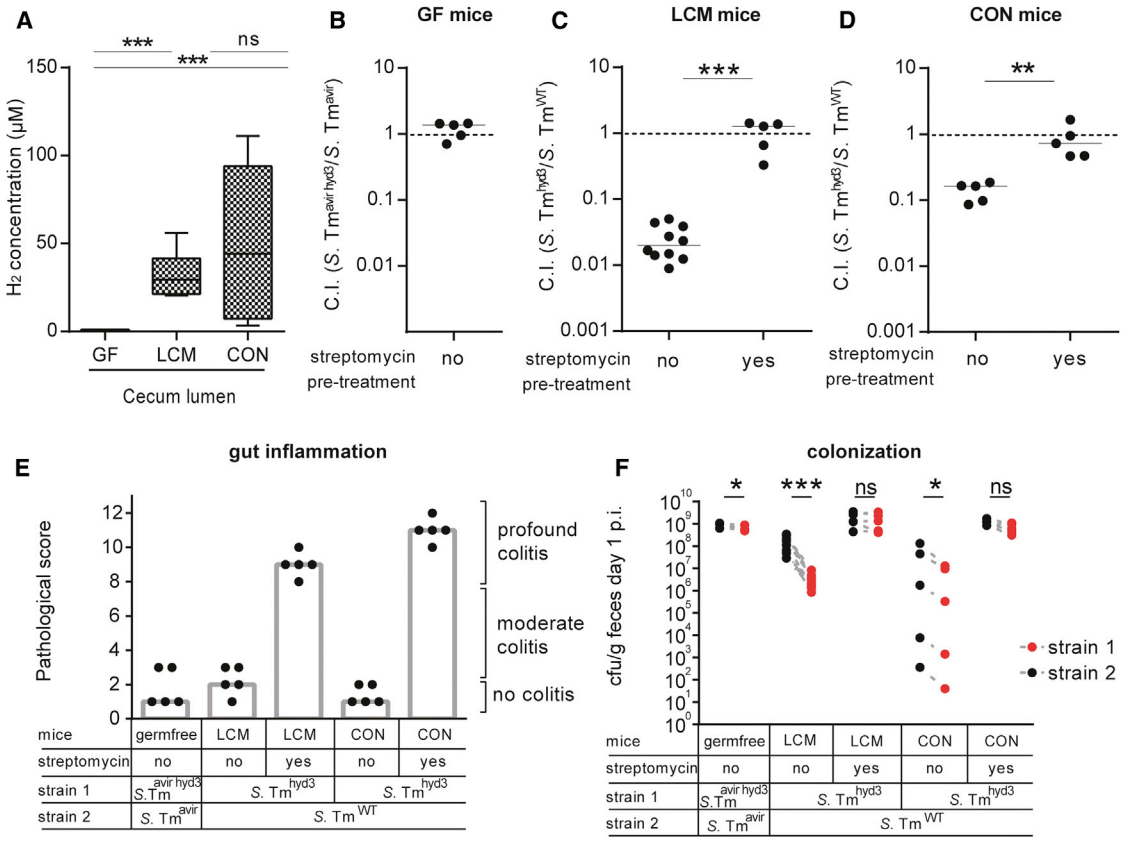

Figure 4. Defective Gut Ecosystem Invasion by *S.* Tm Hydrogenase Mutants Is Linked to Microbiota-Derived H_2

(A) H_2 levels in the cecum lumen. H_2 concentrations were measured at three different positions in the cecum and corrected for electrode crosssensitivity to H_2S (≥3 mice per group) (Experimental Procedures). Box and whiskers plot: the box indicates first and third quartiles, and whiskers denote minimal and maximal measurement readings.

(B) C.I. experiment of *S.* $Tm^{avir\ hyd3}$ versus *S.* Tm^{avir} in five germ-free mice (5×10^7 cfu by gavage; analysis at day 1 p.i.).

(C) C.I. experiment of *S.* Tm^{hyd3} versus *S.* Tm^{WT} in naive LCM mice or streptomycin pretreated animals (10/5 mice per group; 5×10^7 cfu by gavage; analysis at day 1 p.i.).

(D) C.I. experiment of *S.* Tm^{hyd3} versus *S.* Tm^{WT} in naive CON mice or streptomycin pretreated animals (five mice per group; 5×10^7 cfu by gavage; analysis at day 1 p.i.). ns, not significant ($p \geq 0.05$), **$p < 0.01$, ***$p < 0.001$; Mann-Whitney U test.

(E) Pathological scores of the cecal mucosa at day 1 p.i. Cecal tissue sections from the competitive infection experiment shown in (B)–(D) were stained with HE and scored for inflammation.

(F) Bacterial loads of both competing strains at day 1 p.i. were determined by differential plating. ns, not significant ($p > 0.05$), *$p < 0.05$, ***$p < 0.001$; one-tailed Wilcoxon matched pairs signed rank test on paired data (dashed lines).

See also Figure S4 and Table S3.

to be in conflict with earlier work in the oral infection model for typhoid fever (Maier et al., 2004). Upon oral infection, hydrogenase mutants of *S.* Typhimurium ATCC14028 failed to colonize the livers and spleens. Our data may suggest that this attenuation was attributable at least in part to defective growth in the gut, before the bacteria had actually disseminated to systemic sites. This hypothesis would be in line with hydrogenase expression of ATCC14028 in the murine ileum (Zbell et al., 2008). However, we cannot formally exclude that ATCC14028 differs from the SL1344 strain used in our study in being capable of utilizing H_2 in liver and spleen. Such strain-specific differences may affect the adaptation to new hosts. Clearly, *S.* Tm SL1344 requires H_2 only for gut colonization, but not at systemic sites (Figure S3C). This provides a striking example for a central intermediate of microbiota metabolism fuelling pathogen growth at a site occupied by a dense commensal community. Due to the conserved nature of the metabolic network of the gut microbiota, this metabolite will likely be available in any host animal as well as in humans. Thus, H_2 could be regarded as an "Achilles' heel" of microbiota metabolism which can be exploited by *S.* Tm for gut ecosystem invasion.

Molecular hydrogen might affect a number of enteric bacterial infections. This is indicated by genetic evidence for hydrogen-consuming hydrogenases, in vitro data demonstrating roles of hydrogenases in energy conservation, metabolite uptake, and acid resistance by various enteropathogens, including *E. coli*, *Shigella* spp., *Yersinia* spp., and *Campylobacter* spp. (Lamichhane-Khadka et al., 2011; Lamichhane-Khadka et al., 2010; Maier, 2005; Maier et al., 1996; McNorton and Maier, 2012; Zbell et al., 2007; Zbell and Maier, 2009) (Table S2), and by groundbreaking in vivo experimentation on *Helicobacter pylori* (Maier, 2003; Olson and Maier, 2002). The latter requires an

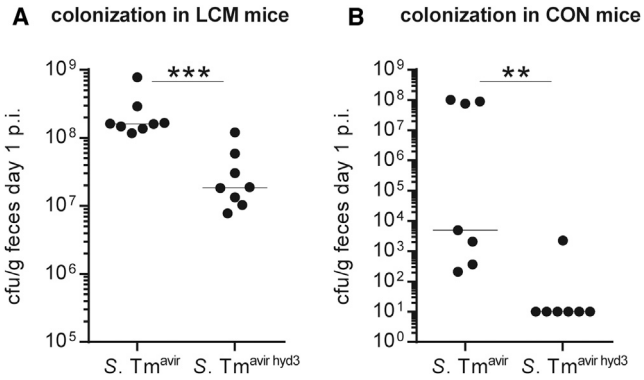

Figure 5. *S.* Tm $^{avir\ hyd3}$ Is Impaired in Colonization of Naive LCM and CON Mice

(A) Eight naive LCM mice or (B) seven naive CON mice were infected with either *S.* Tm^{avir} or *S.* Tm$^{avir\ hyd3}$ (5×10^7 cfu by gavage), and fecal loads were determined at day 1 p.i. $^{**}p < 0.01$, $^{***}p < 0.001$; Mann-Whitney U test.

uptake-type hydrogenase for H_2-dependent colonization of the murine stomach. Interestingly, the H_2 measured at this site was thought (though never shown) to derive from the large-intestinal microbiota. In contrast to the large intestine, which features microbiota densities of 10^{12} cfu/g stool, the stomach is typically colonized by no more than 10^1 microbial cells per gram of content (Sommer and Bäckhed, 2013). Thus, the high diffusibility of H_2 between different organ systems may explain how microbiota-derived H_2 can be tapped not only by pathogens (like *S.* Tm) growing among (and finally outcompeting) the microbiota in the large intestine but also by pathogens colonizing sterile (or almost sterile) sites.

The manipulation of essential metabolite availability may help in preventing pathogen colonization. In fact, as common practice, broiler chicks are treated with attenuated *Salmonella* spp. to reduce the incidence of pathogenic *Salmonella* spp. (Kerr et al., 2013). It is tempting to speculate that this "competitive exclusion" strategy is based at least in part on reduced local availability of H_2. As other enteropathogenic bacteria are also equipped with hydrogenases, H_2 exploitation may represent a common strategy for colonizing the gut. The molecular understanding of the gut ecosystem invasion phase might reveal unique opportunities for thwarting pathogen colonization right from the beginning.

EXPERIMENTAL PROCEDURES

Bacterial Strains

All *S. enterica* serovar Typhimurium strains used in this study are derivatives of the streptomycin-resistant wild-type strain SL1344 (SB300) (Hoiseth and Stocker, 1981) (Supplemental Experimental Procedures). Deletions in the hydrogenase genes were constructed using the lambda/red homologous recombination technique (Datsenko and Wanner, 2000). The genomic region to be deleted was substituted by a *cat* cassette from pKD3 or *aphT* from pKD4. After P22 phage transduction of the antibiotic resistance-substituted region into a clean SB300 strain, the cassette was removed using pCP20 encoded flippase (if indicated). For complementation of the *S.* Tm^{hyb} mutation, the gene SL1344_3112 encoding for a hypothetical protein was substituted by a cat cassette using a lambda/red recombination approach. Substitution of SL1344_3112 with an antibiotic resistance marker did not affect in vivo fitness of the strain (data not shown). P22 phage transduction of the marker including intact *hybABChypO* region into the mutant strain was performed to insert a functional copy of the deleted genomic region into the mutant strain. All constructs were verified by PCR.

Animal Experiments

Animals: CON, LCM, and GF

All animals used in this study are C57BL/6 mice associated with different types of microbiota. Conventional (CON) mice are mice from our in-house colony at the Rodent Center HCI (RCHCI) (Zurich, Switzerland) under specified opportunistic and pathogen-free conditions in individually ventilated cages. LCM (low complex microbiota) mice are ex-germ-free mice which were colonized with the members of the Altered Schaedler flora in 2007 (Stecher et al., 2010) and ever since bred under strict hygienic isolation in a separate breeding room. VLCM (very low complex microbiota) mice are bred at Max-von-Pettenkofer Institute (Munich, Germany) and were generated by inoculating germfree C57BL/6 mice with three strains of the Altered Schaedler flora (ASF361, ASF457, and ASF519; Dewhirst et al., 1999) as pure culture. Germfree C57BL/6 mice were generously provided by the University Hospital Bern. Each experiment was performed at least twice independently, and the data were pooled.

Infection and Competitive Infection Experiments

Single-infection and coinfection experiments were performed in 8- to 12-week-old mice with different composition of the microbiota. Mice were infected as described previously (Barthel et al., 2003). Pretreatment with 20 mg streptomycin was only performed if indicated (i.e., Figures 4C and 4D, right panels; Figures 4E and 4F). For infection or colonization, bacteria were grown for 12 hr in 0.3 M NaCl supplemented LB medium containing the appropriate antibiotic(s), diluted 1:20, and subcultured for 4 hr in the same medium without supplement of antibiotics. Mice were infected with 5×10^7 bacteria by gavage. Freshly collected fecal pellets were harvested, and homogenized in PBS with steel balls in a tissue lyser (QIAGEN) for plating (and frozen for lipocalin-2 ELISA analysis; inflammation marker). Differential plating on MacConkey agar plates (Oxoid) supplemented with the appropriate antibiotics (50 μg/mL streptomycin, 30 μg/mL kanamycin, 30 μg/mL chloramphenicol, 100 μg/mL ampicillin, 12 μg/mL tetracycline) allowed determination of bacterial population size. The competitive index was calculated by dividing the population size of the mutant strain by the population size of the corresponding background strain. The result was corrected for the ratio of both strains in the inoculum. For quantifying live bacterial loads in the organs, mice were sacrificed by cervical dislocation at the indicated time point (untreated, day 1 p.i., day 4 p.i.), and cecal content and mesenteric lymph nodes were recovered. To determine bacterial loads in the mesenteric lymph node, the whole node was homogenized in PBS (0.5% tergitol, 0.5% bovine serum albumin). Minimal detectable values were 10 CFU/g in fecal and cecal content and 10 CFU/organ in the mesenteric lymph node. Parts of the cecal tissue were embedded in OCT (Sakura), and cryosections were prepared and stained with hematoxiline/eosine for pathoscoring. Evaluating submucosal edema, PMN infiltration, presence of goblet cells, and epithelial damage yielded a total score of 0–13 points as described (Hapfelmeier et al., 2008).

Precolonization Experiments

Bacterial strains for precolonization (*S.* Tm^{avir}, *S.* Tm$^{avir\ hyb}$) were grown for 12 hr at 37°C in LB supplemented with 0.3 M NaCl, diluted 1:20 into fresh medium, and subcultured for 4 hr. Animals starved for 4 hr were inoculated with 5×10^7 bacteria by gavage. Twenty-four hours later, fecal pellets were collected to check for successful colonization by plating ($\geq 10^7$ cfu/g feces), and animals were infected with a 1:1 mixture of *S.* Tm^{avir} and *S.* Tm$^{avir\ hyd3}$. Animals were sacrificed 24 hr later, and C.I.s were determined as described above.

In Vivo Screening-type Experiment

Library Generation

The transposon mutant library in *S.* Tm^{WT} was generated as previously described (Chan et al., 2005). Briefly, the suicide plasmid pJA1 (Badarinarayana et al., 2001) was mobilized from *E. coli* SM10 λ*pir* into SL1344 by conjugation for 6 hr in the presence of isopropyl-β-D-thiogalactopyranoside (IPTG) without antibiotic selection. During this time, the plasmid-encoded Tn10 transposase under control of an IPTG-inducible promoter is expressed. The mating reaction was harvested, and dilutions were plated on agar containing

Table 1. Microbiota Metagenomes Show Evidence for H_2-Producing Proteins

	FeFe Hydrogenase		NiFe Hydrogenase		Data Set	Sample Size
Hosts	Small Subunit PF02256	Large Subunit PF02906	Small Subunit PF14720	Large Subunit PF00374	Identifier	Total
Termite	+	+	–	+	Termite	165
Human	+	+	+	+	MetaHit	124
	+	+	+	+	AgeGeo	111
Mouse	–	+	–	–	Lean	1
	–	+	–	–	Obese	1
	+	+	+	+	LCM	1
Dog	+	+	–	+	K9C	6
	+	+	–	–	K9BP	6
Cow	+	+	–	+	Heifer	6
Chicken	–	+	–	–	A	1
	+	+	–	–	B	1

Metagenomes from six different species were analyzed for the presence of large and small subunit genes of FeFe- and NiFe-hydrogenases (Experimental Procedures; for further details, see Table S4). NiFe-hydrogenases comprise both H_2-consuming members and H_2-producing members. In contrast, the FeFe-hydrogenases generally produce (*not* consume) H_2 under anaerobic conditions and are therefore an indicator for hydrogen production within a microbial community (Schwartz and Friedrich, 2006). HmD-like enzymes were not considered, as they are only found in some methanogenic archaea. MG-Rast IDs, 44427013 (termite), 4440285 (chicken cecum A), 4440286 (chicken cecum B), 4444164 (canine K9c), 4444165 (canine K9bp), 4440463 (lean mouse), 4440464 (obese mouse), 4535626.3 and 4535627.3 (LCM mouse), 4448367.3 (cow), http://gutmeta.genomics.org.cn (MetaHIT human gut metagenome study), and 4461119-4461229 (human gut metagenome, "AgeGeo" study). See also Table S4.

200 μg/ml streptomycin and 30 μg/ml kanamycin to select for transposon-containing SL1344 bacteria. Single transposon insertion events per bacterial cells were checked by Southern blot with a probe directed against the transposon sequence (data not shown), and pools of 500 transposon mutants were stocked in peptone (5% glycerol) at −80°C.

Experimental Procedure

The screening-type experiment was adapted from the TraDIS (transposon differential insertion site sequencing) approach which was described previously (Chaudhuri et al., 2009, 2013). Six mice (two independent experiments of three animals each) were infected with a mix containing the pool of 500 transposon mutants and four wild-type isogenic tagged strains (WITS) (Grant et al., 2008) spiked in at a dilution of 1:500 (5×10^7 cfu total in 50 μl PBS). The spiked-in WITS strains contain a 40 nt barcode tag between the two pseudogenes *malX* and *malY* and allowed to check for random loss of subpopulations during the in vivo selection. An aliquot of the inoculum was grown up in LB broth (30 μg/ml kanamycin) and harvested as input pool. Animals were sacrificed at day 4 after infection. Cecal content was harvested, homogenized, and cultured overnight in LB (30 μg/ml kanamycin) to isolate transposon-containing output bacteria and in LB (12 μg/ml tetracycline) to isolate WITS-tagged strains for WITS analysis. Genomic DNA was prepared from input and output samples and fragmented, and RNA was amplified from the gDNA fragments using T7 RNA polymerase. Preparation of 5′ fragment cDNA libraries for 454 Titanium sequencing on a Roche/454 GS FLX sequencer (ca. 450 bp read length) was performed by vertis Biotechnologie AG (Freising, Germany). Briefly, RNA samples were poly(A)-tailed using poly(A) polymerase. An oligo(dT)-adaptor primer and M-MLV-H^- reverse transcriptase was used for first-strand cDNA synthesis. cDNA was amplified with PCR using primers directed to the flanking 5′ transposon and 3′ adaptor primer sequences and a proofreading enzyme. The double-stranded cDNA fragments then had a size of about 200–1,200 bp, were purified using the Agencourt AMPure XP kit (Beckman Coulter Genomics), and were pooled for sequencing.

WITS Analysis

Temporal dynamics of WITS strains during screening experiments were monitored as described previously (Grant et al., 2008). In summary, WITS-tagged bacteria were harvested from enrichment cultures from fecal samples at day 1 after infection or cecum content samples at day 4 postinfection by centrifugation. Genomic bacterial DNA was extracted via the QIAGEN DNA mini kit, and the relative numbers of the four different WITS were determined by real-time PCR quantification using tag-specific primers.

Bioinformatic and Statistical Analysis of the 454 Sequencing Reads

The sequencing vendor provided reads split by barcode for the first sequencing run and pooled reads for the second sequencing run. The pooled sequences were split using a custom python script, using a perfect match criterion to the barcode sequences required. Transposon sequences were trimmed from the reads using Cutadapt version 1.1 (http://journal.embnet.org/index.php/embnetjournal/article/view/200), with a maximum error rate of 10%. The transposon sequence was detected (at least 92% of the reads) in each sample and removed. Untrimmed reads were discarded. Reads were mapped to the SL1344 genome (GenBank entry FQ312003.1) with Bowtie2 (http://www.nature.com/nmeth/journal/v9/n4/full/nmeth.1923.html) version 2.0.0-beta6 using the –local parameter combination for local, gapped alignment, and sorted and converted to bam format using Samtools (http://bioinformatics.oxfordjournals.org/content/25/16/2078.short). Mapping start sites were counted using pysam (http://code.google.com/p/pysam/). Mapped reads starting within several nucleotides of each other were considered to belong to the same transposon insertion site. For each run of contiguous read start sites, the site with the highest coverage was chosen, and the total read count was calculated as the sum of the countiguous reads. Differential representation of the start sites between the input and output samples was estimated using edgeR (http://www.ncbi.nlm.nih.gov/pmc/articles/PMC2796818/), using the generalized linear model framework (http://www.ncbi.nlm.nih.gov/pubmed/22287627) with tagwise dispersions. Counts per million were summed across samples, and start sites with a summed count equal to or less than 25 were excluded. The 30 most significantly attenuated start sites located within operon reading frames were selected for further analysis. Start sites overlapping a gene were annotated.

Lipocalin-2 ELISA

Lipocalin-2 levels were detected in homogenized fecal samples by ELISA using the DuoSet ELISA kit (R&D Systems).

Measurements of Cecal H_2 Concentration Using Clarke-type Microelectrodes

Hydrogen concentrations within the cecal lumen of mice with different microbiotas (CON, LCM, and GF) were measured using microsensors (Unisense, Aarhus, Denmark). The hydrogen microsensor (H-50) with a tip diameter of 50 μm was calibrated in water flushed with a gas mix containing 7% hydrogen at 37°C. This corresponds to a hydrogen concentration of 48.5 μM (Wiesenburg and Guinasso, 1979). Mice were sacrificed; ceca including ileum and

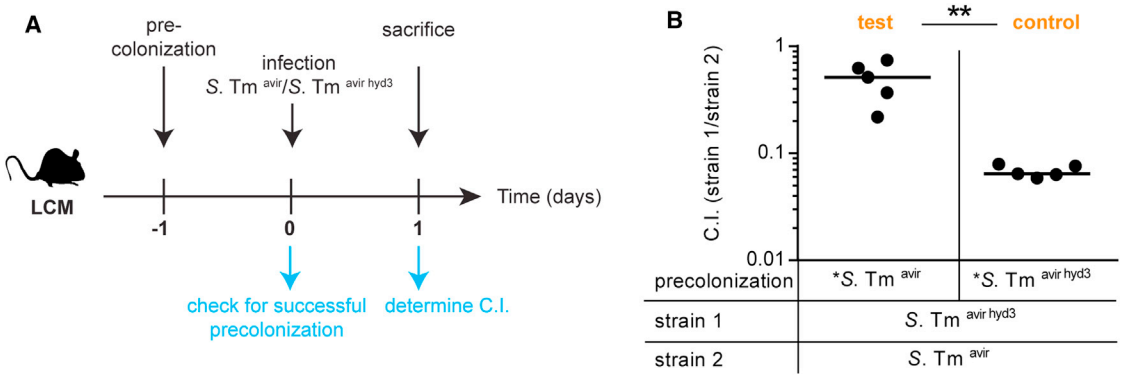

Figure 6. Introducing a Hydrogen Consumer Interferes with *hyb*-Dependent Gut Ecosystem Invasion by *S.* Tm

(A) Experimental strategy.

(B) LCM mice were precolonized with the hydrogen consumer *S.* Tm^{avir} (test) or a mutant incapable to consume hydrogen *S.* $Tm^{avir\ hyd3}$ (control; 5×10^7 cfu by gavage 1 day before infection). Plating verified the precolonization efficiency. Mice were infected with a 1:1 mixture of *S.* Tm^{avir} and *S.* $Tm^{avir\ hyd3}$ (5×10^7 cfu by gavage; five mice per group). C.I.s were determined at day 1 p.i. by differential plating of feces. $^{**}p < 0.01$, Mann-Whitney U test. Asterisk denotes that strains with distinct resistance markers were used for precolonization and for competitive infections.

See also Figure S5.

large intestine were fixed onto a bottom layer of 2% agarose in a petri dish and covered with top agar (45°C, 2% agarose) to fix the intestine as described (Schauer et al., 2012). A 26 G needle was used to pierce holes into the tissue to facilitate the microsensor tip to penetrate into the cecal lumen. After solidification of the top agar, the petri dish was transferred into a 37°C water bath, and microsensor profiles were taken at the prepierced positions. We measured three different spots per cecum: one at the cecal tip, one in the mid-cecum, and one at the opening toward small and large intestine. Please note that the values obtained by this method might be a bit higher than the steady-state levels in the gut of a living animal, as H_2 production is in equilibrium not only with microbial H_2 consumption but also with tissue diffusion, blood-mediated transport, and loss in breath and flatus (Bond and Levitt, 1972; Cummings and Macfarlane, 1991; Levitt et al., 1987).

To exclude artifacts attributable to H_2S, we performed measurements of hydrogen sulfide in parallel in the same mice at the same spots. The H_2S microsensor (H_2S-50) with a tip size of 50 μm was calibrated using an anaerobically prepared stock solution of S^{2-} (~0.01M). The final concentration of the stock solution was determined photometrically as previously described (Siegel, 1965). The H_2S microsensor detects the partial pressure of H_2S gas, a component of the total sulfide equilibrium system. At pH below 4, the equilibrium is shifted in favor of the gas, and all sulfides exist as gaseous H_2S. Therefore, the stock solution was diluted with degased technical buffer pH 1. Calibration values were taken at 37°C by removing the rubber stopper from the diluted calibration solutions (10 μM, 50 μM, and 200 μM), and the microsensor tip was immersed into the solution. We measured a median of 170 μM for CON mice, 63 μM for LCM mice, and 0 μM GF mice. Using these values, we corrected the signals measured with the H_2 microsensor for H_2S interference based on a crosssensititvity of 10% reported by the supplier (Unisense).

Metagenomic Analysis

DNA extraction of microbiota from murine feces of an LCM mouse of our colony was performed in the same way as for 16S rRNA gene sequencing (Supplemental Experimental Procedures). DNA library construction and high-throughput sequencing of the LCM microbiota metagenome were performed by BGI (Shenzhen, China) using Illumina's Hiseq technology (91PE) as previously decribed (Qin et al., 2010). The contigs were assembled using velvet with a k-mer length of 29, and host genomic sequences were filtered out using Bowtie2 and deposited as MG-Rast accession numbers 4535626.3 and 4535627.3.

Other sequences were retrieved from the public databases (Table 1). Nucleotide contig sets of the metagenomic data sets were procured from MG-RAST. These contig sets were prefiltered to remove the host genomic sequences. A six-frame translation was carried out on each of the individual data sets to identify any open reading frames coding for peptides longer than 30 amino acids. Next, a set of four pfam models—PF00374, PF02256, PF14720, and PF02906—was used for identifying homologs of hydrogenase subunits in our data sets. The initial screening was performed using Hmmscan with an value restriction of 0.0001, and these hits were reverse-screened against the entire Pfam HMM database.

Statistical Analysis

The one-sided Wilcoxon matched-pairs signed rank test and the exact Mann-Whitney U test were performed using the software Graphpad Prism Version 6.0 for Windows (GraphPad Software, http://www.graphpad.com). p values of less than 0.05 (two-tailed) were considered as statistically significant. To compare C.I.s to C.I. of inoculi, ratios of strain 1 and strain 2 were compared to the ratio of both strains in the inoculum using an exact Mann-Whitney U test.

Ethical Statement

All animal experiments were reviewed and approved by the Kantonales Veterinäramt, Zürich (license 223/2010 + Ergänzung 9) and are subject to the Swiss animal protection law (TschG).

SUPPLEMENTAL INFORMATION

Supplemental Information includes five figures, four tables, and Supplemental Experimental Procedures and can be found with this article at http://dx.doi.org/10.1016/j.chom.2013.11.002.

ACKNOWLEDGMENTS

We are grateful to the members of the Hardt lab; to Tobias Erb, Andrew Macpherson, Julia Vorholt, and Hauke Hennecke for helpful scientific discussions; to Hans-Joachim Ruscheweyh (Center for Bioinformatics, Tübingen University) for support in 16S sequencing data analysis; to Thomas C. Weber and the RCHCI team (especially Corina Fusaro-Graf and Marion Hermerschmidt) for expert assistance with animal work; and to Manja Barthel and Maria Rita Lecca (FGCZ) for excellent technical support. This work was supported in part by the Swiss National Science Foundation (310030-132997/1 and the Sinergia project CRSII3_136286 to W.-D.H.).

Received: October 8, 2013
Revised: November 1, 2013
Accepted: November 11, 2013
Published: December 11, 2013

REFERENCES

Ackermann, M., Stecher, B., Freed, N.E., Songhet, P., Hardt, W.D., and Doebeli, M. (2008). Self-destructive cooperation mediated by phenotypic noise. Nature *454*, 987–990.

Allen-Vercoe, E., and Woodward, M.J. (1999). Colonisation of the chicken caecum by afimbriate and aflagellate derivatives of Salmonella enterica serotype Enteritidis. Vet. Microbiol. *69*, 265–275.

Badarinarayana, V., Estep, P.W., 3rd, Shendure, J., Edwards, J., Tavazoie, S., Lam, F., and Church, G.M. (2001). Selection analyses of insertional mutants using subgenic-resolution arrays. Nat. Biotechnol. *19*, 1060–1065.

Barthel, M., Hapfelmeier, S., Quintanilla-Martínez, L., Kremer, M., Rohde, M., Hogardt, M., Pfeffer, K., Rüssmann, H., and Hardt, W.D. (2003). Pretreatment of mice with streptomycin provides a Salmonella enterica serovar Typhimurium colitis model that allows analysis of both pathogen and host. Infect. Immun. *71*, 2839–2858.

Bond, J.H., Jr., and Levitt, M.D. (1972). Use of pulmonary hydrogen (H 2) measurements to quantitate carbohydrate absorption. Study of partially gastrectomized patients. J. Clin. Invest. *51*, 1219–1225.

Carbonero, F., Benefiel, A.C., and Gaskins, H.R. (2012). Contributions of the microbial hydrogen economy to colonic homeostasis. Nat. Rev. Gastroenterol. Hepatol. *9*, 504–518.

Chan, K., Kim, C.C., and Falkow, S. (2005). Microarray-based detection of Salmonella enterica serovar Typhimurium transposon mutants that cannot survive in macrophages and mice. Infect. Immun. *73*, 5438–5449.

Chaudhuri, R.R., Peters, S.E., Pleasance, S.J., Northen, H., Willers, C., Paterson, G.K., Cone, D.B., Allen, A.G., Owen, P.J., Shalom, G., et al. (2009). Comprehensive identification of Salmonella enterica serovar typhimurium genes required for infection of BALB/c mice. PLoS Pathog. *5*, e1000529.

Chaudhuri, R.R., Morgan, E., Peters, S.E., Pleasance, S.J., Hudson, D.L., Davies, H.M., Wang, J., van Diemen, P.M., Buckley, A.M., Bowen, A.J., et al. (2013). Comprehensive assignment of roles for Salmonella typhimurium genes in intestinal colonization of food-producing animals. PLoS Genet. *9*, e1003456.

Cotillard, A., Kennedy, S.P., Kong, L.C., Prifti, E., Pons, N., Le Chatelier, E., Almeida, M., Quinquis, B., Levenez, F., Galleron, N., et al.; ANR MicroObes Consortium (2013). Dietary intervention impact on gut microbial gene richness. Nature *500*, 585–588.

Craven, S.E. (1994). Altered colonizing ability for the ceca of broiler chicks by lipopolysaccharide-deficient mutants of Salmonella typhimurium. Avian Dis. *38*, 401–408.

Cummings, J.H., and Macfarlane, G.T. (1991). The control and consequences of bacterial fermentation in the human colon. J. Appl. Bacteriol. *70*, 443–459.

Datsenko, K.A., and Wanner, B.L. (2000). One-step inactivation of chromosomal genes in Escherichia coli K-12 using PCR products. Proc. Natl. Acad. Sci. USA *97*, 6640–6645.

Dewhirst, F.E., Chien, C.C., Paster, B.J., Ericson, R.L., Orcutt, R.P., Schauer, D.B., and Fox, J.G. (1999). Phylogeny of the defined murine microbiota: altered Schaedler flora. Appl. Environ. Microbiol. *65*, 3287–3292.

Endt, K., Stecher, B., Chaffron, S., Slack, E., Tchitchek, N., Benecke, A., Van Maele, L., Sirard, J.C., Mueller, A.J., Heikenwalder, M., et al. (2010). The microbiota mediates pathogen clearance from the gut lumen after non-typhoidal Salmonella diarrhea. PLoS Pathog. *6*, e1001097.

Fischbach, M.A., and Sonnenburg, J.L. (2011). Eating for two: how metabolism establishes interspecies interactions in the gut. Cell Host Microbe *10*, 336–347.

Flint, H.J., Bayer, E.A., Rincon, M.T., Lamed, R., and White, B.A. (2008). Polysaccharide utilization by gut bacteria: potential for new insights from genomic analysis. Nat. Rev. Microbiol. *6*, 121–131.

Food and Agriculture Organization of the United Nations (2002). W.H.O. (Risk Assessments of Salmonella in Eggs and Broiler Chickens).

Grant, A.J., Restif, O., McKinley, T.J., Sheppard, M., Maskell, D.J., and Mastroeni, P. (2008). Modelling within-host spatiotemporal dynamics of invasive bacterial disease. PLoS Biol. *6*, e74.

Hapfelmeier, S., Stecher, B., Barthel, M., Kremer, M., Müller, A.J., Heikenwalder, M., Stallmach, T., Hensel, M., Pfeffer, K., Akira, S., and Hardt, W.D. (2005). The Salmonella pathogenicity island (SPI)-2 and SPI-1 type III secretion systems allow Salmonella serovar typhimurium to trigger colitis via MyD88-dependent and MyD88-independent mechanisms. J. Immunol. *174*, 1675–1685.

Hapfelmeier, S., Müller, A.J., Stecher, B., Kaiser, P., Barthel, M., Endt, K., Eberhard, M., Robbiani, R., Jacobi, C.A., Heikenwalder, M., et al. (2008). Microbe sampling by mucosal dendritic cells is a discrete, MyD88-independent step in DeltainvG S. Typhimurium colitis. J. Exp. Med. *205*, 437–450.

Hoiseth, S.K., and Stocker, B.A. (1981). Aromatic-dependent Salmonella typhimurium are non-virulent and effective as live vaccines. Nature *291*, 238–239.

Ilg, K., Endt, K., Misselwitz, B., Stecher, B., Aebi, M., and Hardt, W.D. (2009). O-antigen-negative Salmonella enterica serovar Typhimurium is attenuated in intestinal colonization but elicits colitis in streptomycin-treated mice. Infect. Immun. *77*, 2568–2575.

Kaiser, P., Diard, M., Stecher, B., and Hardt, W.D. (2012). The streptomycin mouse model for Salmonella diarrhea: functional analysis of the microbiota, the pathogen's virulence factors, and the host's mucosal immune response. Immunol. Rev. *245*, 56–83.

Kerr, A.K., Farrar, A.M., Waddell, L.A., Wilkins, W., Wilhelm, B.J., Bucher, O., Wills, R.W., Bailey, R.H., Varga, C., McEwen, S.A., and Rajić, A. (2013). A systematic review-meta-analysis and meta-regression on the effect of selected competitive exclusion products on Salmonella spp. prevalence and concentration in broiler chickens. Prev. Vet. Med. *111*, 112–125.

Lamichhane-Khadka, R., Kwiatkowski, A., and Maier, R.J. (2010). The Hyb hydrogenase permits hydrogen-dependent respiratory growth of Salmonella enterica serovar Typhimurium. MBio. *1*, e00284-10.

Lamichhane-Khadka, R., Frye, J.G., Porwollik, S., McClelland, M., and Maier, R.J. (2011). Hydrogen-stimulated carbon acquisition and conservation in Salmonella enterica serovar Typhimurium. J. Bacteriol. *193*, 5824–5832.

Le Chatelier, E., Nielsen, T., Qin, J., Prifti, E., Hildebrand, F., Falony, G., Almeida, M., Arumugam, M., Batto, J.M., Kennedy, S., et al.; MetaHIT consortium (2013). Richness of human gut microbiome correlates with metabolic markers. Nature *500*, 541–546.

Levitt, M.D., Hirsh, P., Fetzer, C.A., Sheahan, M., and Levine, A.S. (1987). H2 excretion after ingestion of complex carbohydrates. Gastroenterology *92*, 383–389.

Ley, R.E., Lozupone, C.A., Hamady, M., Knight, R., and Gordon, J.I. (2008). Worlds within worlds: evolution of the vertebrate gut microbiota. Nat. Rev. Microbiol. *6*, 776–788.

Maier, R.J. (2003). Availability and use of molecular hydrogen as an energy substrate for Helicobacter species. Microbes Infect. *5*, 1159–1163.

Maier, R.J. (2005). Use of molecular hydrogen as an energy substrate by human pathogenic bacteria. Biochem. Soc. Trans. *33*, 83–85.

Maier, R.J., Fu, C., Gilbert, J., Moshiri, F., Olson, J., and Plaut, A.G. (1996). Hydrogen uptake hydrogenase in Helicobacter pylori. FEMS Microbiol. Lett. *141*, 71–76.

Maier, R.J., Olczak, A., Maier, S., Soni, S., and Gunn, J. (2004). Respiratory hydrogen use by Salmonella enterica serovar Typhimurium is essential for virulence. Infect. Immun. *72*, 6294–6299.

McNorton, M.M., and Maier, R.J. (2012). Roles of H2 uptake hydrogenases in Shigella flexneri acid tolerance. Microbiology *158*, 2204–2212.

Ng, K.M., Ferreyra, J.A., Higginbottom, S.K., Lynch, J.B., Kashyap, P.C., Gopinath, S., Naidu, N., Choudhury, B., Weimer, B.C., Monack, D.M., and Sonnenburg, J.L. (2013). Microbiota-liberated host sugars facilitate post-antibiotic expansion of enteric pathogens. Nature *502*, 96–99.

Olson, J.W., and Maier, R.J. (2002). Molecular hydrogen as an energy source for Helicobacter pylori. Science *298*, 1788–1790.

Qin, J., Li, R., Raes, J., Arumugam, M., Burgdorf, K.S., Manichanh, C., Nielsen, T., Pons, N., Levenez, F., Yamada, T., et al.; MetaHIT Consortium (2010). A human gut microbial gene catalogue established by metagenomic sequencing. Nature *464*, 59–65.

Schauer, C., Thompson, C.L., and Brune, A. (2012). The bacterial community in the gut of the Cockroach Shelfordella lateralis reflects the close evolutionary relatedness of cockroaches and termites. Appl. Environ. Microbiol. *78*, 2758–2767.

Schwartz, E., and Friedrich, B. (2006). The H2-metabolizing prokaryoes. In The Prokaryotes: A Handbook on the Biology of Bacteria, Vol. 2, Ecophysiology and Biochemistry, M. Dworkin, ed. (New York: Springer).

Siegel, L.M. (1965). A Direct Microdetermination for Sulfide. Anal. Biochem. *11*, 126–132.

Sommer, F., and Bäckhed, F. (2013). The gut microbiota—masters of host development and physiology. Nat. Rev. Microbiol. *11*, 227–238.

Stecher, B., and Hardt, W.D. (2011). Mechanisms controlling pathogen colonization of the gut. Curr. Opin. Microbiol. *14*, 82–91.

Stecher, B., Hapfelmeier, S., Müller, C., Kremer, M., Stallmach, T., and Hardt, W.D. (2004). Flagella and chemotaxis are required for efficient induction of Salmonella enterica serovar Typhimurium colitis in streptomycin-pretreated mice. Infect. Immun. *72*, 4138–4150.

Stecher, B., Robbiani, R., Walker, A.W., Westendorf, A.M., Barthel, M., Kremer, M., Chaffron, S., Macpherson, A.J., Buer, J., Parkhill, J., et al. (2007). Salmonella enterica serovar typhimurium exploits inflammation to compete with the intestinal microbiota. PLoS Biol. *5*, 2177–2189.

Stecher, B., Barthel, M., Schlumberger, M.C., Haberli, L., Rabsch, W., Kremer, M., and Hardt, W.D. (2008). Motility allows S. Typhimurium to benefit from the mucosal defence. Cell. Microbiol. *10*, 1166–1180.

Stecher, B., Chaffron, S., Käppeli, R., Hapfelmeier, S., Freedrich, S., Weber, T.C., Kirundi, J., Suar, M., McCoy, K.D., von Mering, C., et al. (2010). Like will to like: abundances of closely related species can predict susceptibility to intestinal colonization by pathogenic and commensal bacteria. PLoS Pathog. *6*, e1000711.

van Opijnen, T., and Camilli, A. (2013). Transposon insertion sequencing: a new tool for systems-level analysis of microorganisms. Nat. Rev. Microbiol. *11*, 435–442.

Wiesenburg, D.A., and Guinasso, N.L. (1979). Equilibrium solubilities of methane, carbon monoxide and hydrogen in water and sea water. J. Chem. Eng. Data *24*, 356–360.

Willing, B.P., Russell, S.L., and Finlay, B.B. (2011). Shifting the balance: antibiotic effects on host-microbiota mutualism. Nat. Rev. Microbiol. *9*, 233–243.

Winter, S.E., Lopez, C.A., and Bäumler, A.J. (2013). The dynamics of gut-associated microbial communities during inflammation. EMBO Rep. *14*, 319–327.

Zbell, A.L., and Maier, R.J. (2009). Role of the Hya hydrogenase in recycling of anaerobically produced H2 in Salmonella enterica serovar Typhimurium. Appl. Environ. Microbiol. *75*, 1456–1459.

Zbell, A.L., Benoit, S.L., and Maier, R.J. (2007). Differential expression of NiFe uptake-type hydrogenase genes in Salmonella enterica serovar Typhimurium. Microbiology *153*, 3508–3516.

Zbell, A.L., Maier, S.E., and Maier, R.J. (2008). Salmonella enterica serovar Typhimurium NiFe uptake-type hydrogenases are differentially expressed in vivo. Infect. Immun. *76*, 4445–4454.